Development of High Power Models of Four-Slot Annular Coupled Structure

T. Kageyama, Y. Morozumi, K. Yoshino and Y. Yamazaki
KEK, National Laboratory for High Energy Physics
Oho 1-1, Tsukuba-shi, Ibaraki-ken 305, Japan

Abstract

A $\pi/2$-mode standing-wave linac (f=1.296GHz) of an Annular Coupled Structure (ACS) has been developed for the 1-GeV proton linac of the Japanese Hadron Project (JHP). This ACS has four coupling slots between accelerating and coupling cells in order to suppress higher order mode mixing with the $\pi/2$ coupling mode. High-β(β=v/c=0.78) and low-β(0.52) prototypes were constructed and tested up to each design RF power. Concerning the effect of the coupling slots on the fields of a coupled-cavity linac, it was found that the slot configuration of the side-coupled structure (SCS) tilts the accelerating field. On the other hand, the four-slot configuration of the ACS gives an almost axially symmetric accelerating field to the beam.

I. INTRODUCTION

In a $\pi/2$ ACS [1], accelerating cells and non-excited annular coupling cells are alternately located as shown in Fig. 1. It is the annular coupling cell that typifies the RF properties of the ACS. An annular cavity has TM dipole and quadrupole modes near the lowest TM monopole mode used as the $\pi/2$ coupling mode. It makes the coupling mode very sensitive to breakdown of the axial symmetry of the annular cavity [2-4]. But, the axial symmetry is inevitably broken by the coupling slots. This RF property had prevented the ACS from being put to practical use.

Increasing the number of coupling slots and reducing the individual slot size is expected to keep the breakdown of axial symmetry as small as possible. In order to study the feasibility of a multi-slot ACS, four-slot and eight-slot ACS cold models were made and their RF properties were measured. The following results were obtained [4]:

- With the four-slot configuration, the axial symmetry can be sufficiently restored to suppress higher order mode mixing with the coupling mode.
- With the eight-slot configuration, no improvements were found, compared with the four-slot configuration.
- To attain the same coupling constant, the total arc length of slots, defined by the arc length of one slot multiplied by the number of slots, becomes longer as the number of coupling slots increases.

Considering the structural strength and thermal conductivity of the ACS cavity, the four-slot configuration is a practical solution.

The results of the cold model tests encouraged us to develop high-power models of the four-slot ACS. Three high-β(β=0.78) tanks and one low-β (β=0.52) tank have been constructed and tested so far. Results of the RF measurements and high-power tests for the high-β tanks were reported in References [5, 6].

As an efficient $\pi/2$-mode coupled-cavity structure, the side-coupled structure (SCS) [7] is well known and has been used in many linacs. Its shunt impedance is higher than that of the four-slot ACS by ~5%. Why should we develop the ACS while an efficient SCS linac is already available? The reason is as follows: For future high-brightness linacs, we need an accelerating structure that never deteriorates the beam quality and has reasonable efficiency. Distortion of the accelerating field due to the coupling slots becomes a serious problem in high-brightness linacs [8]. Recently, we have found by numerical simulations that the SCS slot configuration tilts the accelerating field in the way that the TM010 mode is mixed with a TE111-like mode [6]. The accelerating mode mixed with a TE-dipole mode kicks the beam in a transverse direction and may deteriorate the beam quality. On the other hand, the slot configuration of the four slot ACS mixes the accelerating mode with a TE-octupole mode. However, the field strength of the octupole component is negligibly small near the beam axis. Therefore, the four-slot ACS is expected to give an axially symmetric accelerating field to the beam. That motivated us to carry out the R&D of the four-slot ACS for future high-brightness linacs.

II. HIGH-POWER MODELS

A. Structure

For high-β prototypes (β=0.78), two 5-cell tanks with the staggered slot configuration (type S) and one 5-cell tank with the uniform slot configuration (type U) were constructed. Here, 5-cell means 5-accelerating-cell. For type S, the azimuthal orientation of coupling slot is rotated by 45 degrees from segment to segment as shown in Fig. 1, while the slot orientation is uniform for type U. Comparing the two configurations with the same slot size, type S gives a larger coupling factor and a higher shunt impedance than type U [6]. As a low-β prototype, a 7-cell tank (β=0.52) with the slot configuration of type S was constructed.

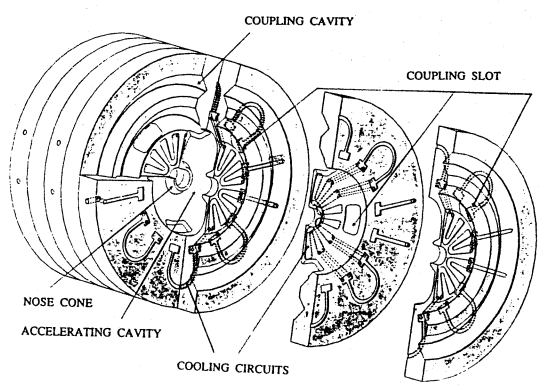

Fig. 1 A cutaway view of a four-slot ACS cavity with the staggered slot configuration. The slot orientation is rotated by 45 degrees from segment to segment.

Table 1
Design and measured parameters for the low-β and high-β prototypes

frequency	1.296 GHz	
duty factor	3 %	
pulse width	600 μs	
repetition rate	50 Hz	
	low-β prototype	high-β prototype
$\beta = v/c$	0.52	0.78
E_0T	3.0 MV/m	3.5 MV/m
RF peak power	18 kW/cell	26 kW/cell
coupling constant	0.052 measured	0.056 measured
Q	1.5×10^4 / 1.8×10^4	1.9×10^4 / 2.4×10^4
$R(=ZT^2)$ MΩ/m	30 / 37	42 / 54
R/Q Ω/cell	120 / 124	201 / 205
	measured / SuperFish	*measured / SuperFish*

Table 1 gives design and measured RF parameters for the low-β and high-β tanks with the slot configuration of type S. The shape of the accelerating cell was optimized to give a high shunt impedance, and the coupling cavity was designed like a resonant ring of ridged waveguide to make the tank diameter as small as possible.

The cavity parts were machined from oxygen-free copper (OFC) using a super-precision lathe and a milling machine. Four coupling slots were bored at the wall between the accelerating and coupling cells. At each side of the coupling slot, the edge was tapered so as to increase the magnetic coupling. Before brazing, each of the accelerating and coupling cells was tuned to the design frequency within ±100 kHz by fine machining. Finally, the cavity parts were stacked and brazed in a vacuum furnace to form a tank.

Concerning the water cooling, the average power dissipation per accelerating cell amounts to 540 W for the low-β tank, and 780 W for the high-β one. In order to reduce the thermal detunig, the nosecone region is directly cooled by water circuits in the septum between accelerating cells [9].

Figure 2 shows a schematic drawing of a setup for high power test. This setup consists of the low-β tank (left side) and the high-β one (right side) coupled via a bridge coupler. The bridge coupler is a 5-cell disk-loaded structure and has an input iris port at the middle cell [10].

B. *RF Properties*

Figure 3 shows the electric field distribution on the beam axis for excitation in the $\pi/2$ mode, measured by bead perturbation for the setup in Fig. 2. This field distribution was obtained without retuning of the accelerating cells after brazing. For each of the high-β and low-β tanks, the field distribution is uniform within ±0.5% except the end cells, the electric fields of which are higher by ~5%.

Measured RF parameters, Q, R(=ZT²), R/Q, and coupling constant are listed in Table 1, together with the theoretical values calculated using SUPERFISH. For the high-β tank with a coupling constant of 5.6%, the shunt impedance is reduced by 22% compared with the theoretical value. This reduction consists of two parts: a reduction of 4% coming from surface imperfections of the cavity wall; the remaining 18% is due to the coupling slots. For the low-β tank, the coupling constant of which is 5.2%, the shunt impedance is reduced by 19%, where 4% is due to the surface imperfections and 15% due to the coupling slots.

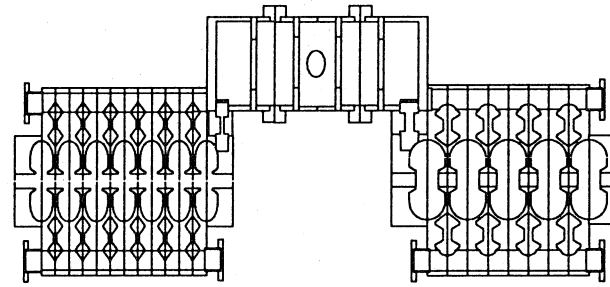

Fig. 2 A schematic drawing of a setup for high power test.

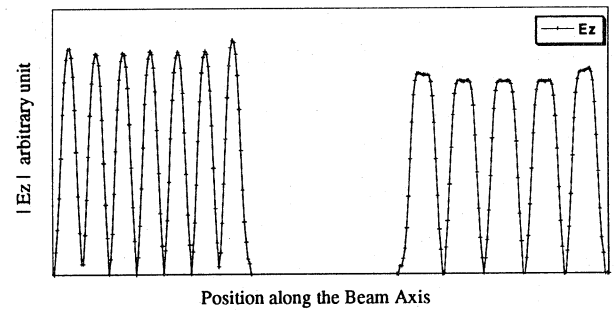

Fig. 3 The electric field distribution on the beam axis for excitation in the $\pi/2$ accelerating mode, measured by bead perturbation for the setup in Fig. 2.

C. *High-Power Test*

A series of high-power tests were carried out with the high-β and low-β prototypes, changing the combination of tanks. RF power was supplied by a pulsed klystron of TH2104A by THOMSON-CSF. For each test, the first RF processing was carried out at a low duty factor of 0.1% (100μs × 10Hz). Next, the duty factor was increased step by step up to 2.75% (550μs×50Hz). Each ACS tank was evacuated with a 300-l/s turbo-molecular pump, and RF processing was carried out keeping the vacuum pressure level below 2×10^{-6} Torr. The thermal detuning was compensated with three movable tuners installed at the bridge coupler.

At a duty factor of 2.75% (550μs × 50Hz), each of the high-β and low-β prototypes was successfully conditioned up to a peak power level 1.5 times as high as the rated peak power in Table 1.

III. DISTORTION OF ACCELERATING FIELD DUE TO COUPLING SLOTS

We have analyzed the field distortion of the accelerating mode caused by the SCS slot configuration, together with that by the four-slot configuration of the ACS. The preliminary results were reported in Ref. [6].

The analyses were carried out using MAFIA as follows:

- First, the electromagnetic fields were calculated for the accelerating mode of each coupled-cavity structure.
- Second, the electromagnetic fields were calculated for the axially symmetric single-cell cavity without coupling slots.
- Finally, the distortion of the accelerating field was obtained by subtracting the electromagnetic fields of the single-cell cavity from those of each coupled-cavity structure.

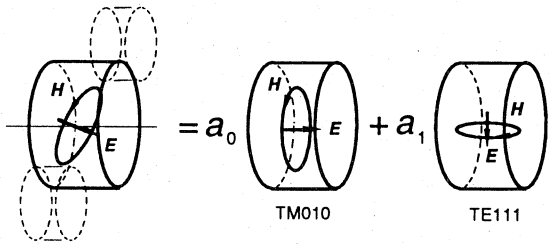

Fig. 4 A schematic drawing showing how the SCS slot configuration tilts the accelerating field.

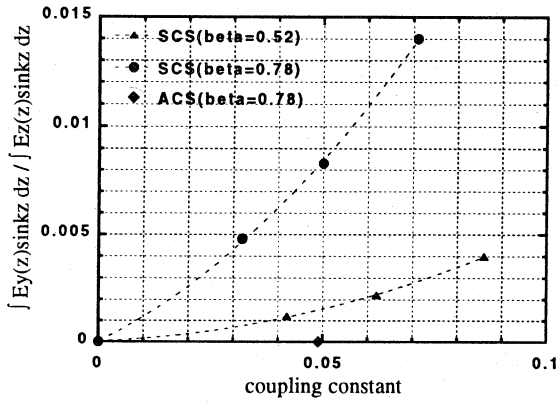

Fig. 5 For two SCS cases with different βs, the ratio of the transverse kick to the longitudinal acceleration is plotted as a function of the coupling constant, compared with that for a four-slot ACS.

From these simulations, we have found that the SCS slot configuration tilts the accelerating field from the beam axis. An accelerating cell of the SCS has one of the two adjacent coupling cells mounted on the top and the other attached to the bottom, as shown in Fig. 4. This slot configuration is asymmetric with respect to the horizontal plane, and tilts the accelerating field. In the language of the perturbation theory, this tilt is caused in the way that the TM010 mode is mixed with a TE111-like mode, which is schematically shown in Fig. 4.

Next, we calculated how much the beam is kicked in a transverse direction by the SCS accelerating field mixed with a TE111-like mode when the beam traverses the accelerating gap. Simulations were carried out for two SCS cases: one is for β=0.52 and the other for β=0.78. Figure 5 shows the ratio of the transverse kick to the longitudinal acceleration, plotted as a function of the coupling constant k. The ratio at $k=0$ is for the axially symmetric single-cell cavity. For example, the SCS of β=0.78 with a coupling constant of 0.05 gives a transverse kick ratio of 8×10^{-3}, which can not be negligible. But, fortunately, the direction of the transverse kick by the tilted accelerating field is reversed from gap to gap. Therefore, the transverse kicks by two adjacent gaps cancel out. However, this counterbalance is assured only when there are no errors in the field amplitude or phase and the beam dynamics remains linear.

Comparing the two SCS cases, the transverse kick by the SCS of β=0.78 is more than five times as large as that by the SCS of β =0.5. This can be well explained as follows: The TE111 frequency depends on the cell length, and becomes lower as the cell becomes longer. According to the perturbation theory, the TE111-mode mixing increases as its frequency comes down toward the accelerating-mode frequency 1.3 GHz from 3.3 GHz for β = 0.52 to 2.3 GHz for β = 0.78.

For the four-slot configuration of the ACS, it was found that the accelerating field is mixed with a TE-octupole mode. However, the field strength of the octupole component is negligibly small near the beam axis. Therefore, the four-slot ACS gives a distortion-free accelerating field to the beam. Figure 5 shows that the transverse kick ratio of the ACS with k = 0.05 is almost equal to zero.

IV. CONCLUSION

High-β and low-β prototypes of the four-slot ACS were constructed and successfully tested up to each design RF power. Due to the coupling slots, the shunt impedance was reduced by 15% for the low-β tank, and by 18% for the high-β one.

Numerical simulations using MAFIA were carried out for the SCS and the four-slot ACS in order to study the field distortion caused by the coupling slots:

- The SCS slot configuration tilts the accelerating field from the beam axis. This tilt is caused in the way that the accelerating mode is mixed with a TE111-like mode, and the mixing increases as the accelerating cell becomes longer.
- On the other hand, the four-slot ACS has an almost axially symmetric accelerating field near the beam axis.

The four-slot ACS, which has a distortion-free accelerating field and a reasonably high shunt impedance, is promising for future high-brightness linacs.

V. REFERENCES

[1] V.G. Andreev et al., "Study of High-Energy Proton Linac Structures", Proc. 1972 Proton Linac Conf., pp. 114-118, 1972.
[2] R.A. Hoffswell and R.M. Laszewski, "Higher Modes in the Coupling Cells of Coaxial and Annular-Ring Coupled Linac Structure", IEEE Trans. on Nucl. Sci., Vol. 30, pp. 3588-3589, 1983.
[3] R.K. Cooper et al., "Radio-Frequency Structure Development for the Los Alamos/NBS Racetrack Microtron", Preprint LA-UR-83-95, 1983.
[4] T. Kageyama et al., "A New Annular Coupled Structure Suppressing Higher Order Modes' Mixing with the π/2 Coupling Mode", Part. Accel., Vol. 32, pp. 33-38, 1990.
[5] T. Kageyama et al., "A High-Power Model of the ACS Cavity", Proc. 1990 Linac Conf., Albuquerque, USA, LA-12004-C, pp. 150-152, 1990.
[6] T. Kageyama et al., "Development of Annular Coupled Structure", Proc. 1992 Linac Conf., Ottawa, Ontario, Canada, AECL-10728, Vol. 2, pp. 456-458, 1990.
[7] E.A. Knapp, B.C. Knapp, and J.M. Potter, Rev. Sci. Instr., Vol. 39, pp. 979-991, 1968.
[8] R.L. Sheffield et al., "Physics Design of the High Brightness Linac for the Advanced Free-Electron Laser Initiative at Los Alamos", Nucl. Instr. and Meth., Vol. A318, pp. 282-289, 1992.
[9] K. Yoshino et al., "Studies on Water-Cooling of an ACS High-Power Model" (in Japanese), Proc. 1991 Linac Meeting in Japan, Tokyo, pp. 242-244, 1991.
[10] Y. Morozumi et al., "Multi-Cavity Bridge Coupler", Proc. 1990 Linac Conf., Albuquerque, USA, LA-12004-C, pp. 153-155, 1990.